J|A|C|S COMMUNICATIONS

Published on Web 06/17/2010

Two-Dimensional Bipolar Electrochemistry

Stephen E. Fosdick, John A. Crooks, Byoung-Yong Chang, and Richard M. Crooks*

Department of Chemistry and Biochemistry, Center for Electrochemistry, and the Center for Nano- and Molecular Science and Technology, The University of Texas at Austin, University Station, A5300, Austin, Texas 78712-0165

Received April 29, 2010; E-mail: crooks@cm.utexas.edu

Abstract: This paper introduces the concept of two-dimensional bipolar electrochemistry and discusses its principle of operation. The interesting new result is that electrochemical reactions can be localized at particular locations on the perimeter of a two-dimensional bipolar electrode (2D-BPE), configured at the intersection of two orthogonal microfluidic channels, by controlling the electric field within the contacting electrolyte solution. Experimentally determined maps of the electric field in the vicinity of the 2D-BPEs are in semiquantitative agreement with finite element simulations.

Here we introduce the concept of two-dimensional bipolar electrochemistry and discuss its principles of operation. The interesting new result is that electrochemical reactions can be localized at particular locations on the perimeter of a two-dimensional bipolar electrode (2D-BPE) by controlling the electric field within the contacting electrolyte solution. This construct is conceptually distinct from the types of one-dimensional BPEs that we[1−4] and others[5−9] have reported previously, and it opens up the possibility of creating an electrochemical array comprised of a single electrode. Such systems might find applications in chemical sensing[1−3] or in materials synthesis and characterization.[8]

First consider the case of a simple, one-dimensional BPE.[4] When a voltage (E_{tot}) is applied between two driving electrodes present in reservoirs at either end of a single microfluidic channel filled with an electrolyte solution, an electric field is induced within the channel. If an electronically conductive wire of sufficient length is present within the channel, and if E_{tot} is sufficiently high, then faradaic electrochemical reactions will take place at either end of the wire, even though there is no direct electrical connection to it.[4] In this case, the wire is called a BPE, and the fraction of E_{tot} that is dropped in solution over the BPE is defined as ΔE_{elec}.

While the potential difference between the two ends of a BPE and the contacting solution can be conveniently controlled, measurement of current induced in the BPE is more problematic. Some time ago, however, we resolved this difficulty by coupling the electrochemical reaction at the cathodic pole of the BPE to a light-emitting reaction at the anodic pole. Specifically, we used electrogenerated chemiluminescence (ECL), produced by the simultaneous oxidation of $Ru(bpy)_3^{2+}$ and tri-*n*-propylamine (TPrA), to report the rate of the cathodic process.[10] This is an effective strategy because the rates of the faradaic reactions at the two poles of the BPE must be the same.[4] We employ the same approach here.

Now consider the 2D-BPE configuration shown in Scheme 1. It consists of a planar electrode situated at the intersection of two orthogonal microfluidic channels. When driving voltages (E_{tot1} and E_{tot2}) are independently applied across the two channels, the resulting field is the vector sum of the individual fields in the microfluidic channels. Accordingly, the magnitude of the interfacial potential difference between the solution and the BPE, which is the driving force for electrochemical reactions, is a function of location.[4] This provides a means to focus electrochemical reactions at specific points on a 2D-BPE.

Scheme 1

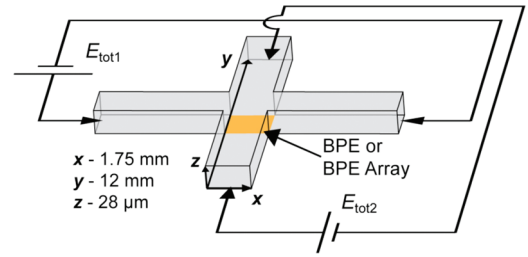

Figure 1a is an optical micrograph of the crossing point of the two channels illustrated in Scheme 1; the light area is the Au BPE, and the polydimethylsiloxane (PDMS) channels are delineated by dashed white lines in the corners of the image. For the experiments described here, the channels were filled with aqueous, air-saturated 5.0 mM $Ru(bpy)_3^{2+}$, 25 mM TPrA, and 0.1 M phosphate buffer (pH 6.9). Under these conditions, ECL is emitted at the anodic pole when oxygen and water reduction occur at the cathodic pole. We have previously shown that ΔE_{elec} must exceed ~1.3 V for ECL emission to be observed under these conditions.[4]

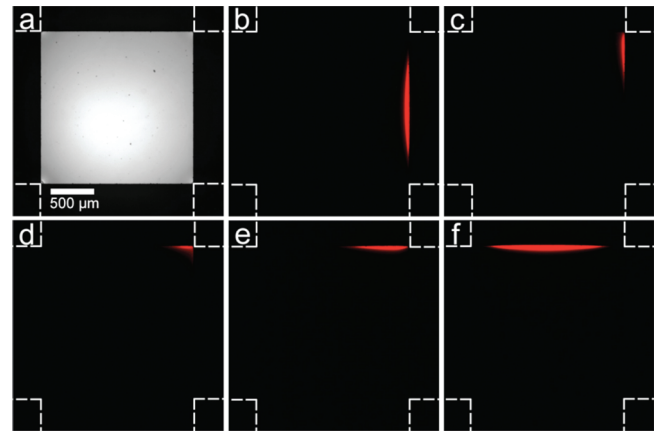

Figure 1. (a) Optical micrograph of the 1.75 × 1.75 mm square BPE illustrated in Scheme 1. The remaining frames show false-color the ECL intensity resulting from application of E_{tot1} and E_{tot2} values of (b) 20.0 and 0 V; (c) 17.3 and 10.0 V; (d) 14.2 and 14.2 V; (e) 10.0 and 17.3 V; and (f) 0 and 20.0 V, respectively.

Figure 1b is a luminescence micrograph showing the red ECL emission when the total voltage applied across the horizontal channel (E_{tot1}, Scheme 1) is 20.0 V and E_{tot2} = 0 V, which is equivalent to $\Delta E_{elec} \approx 2.5$ V. In this case, ECL is emitted just at the right edge of the BPE. However, when a driving voltage is applied to both channels, such that the vector sum remains

10.1021/ja103667y

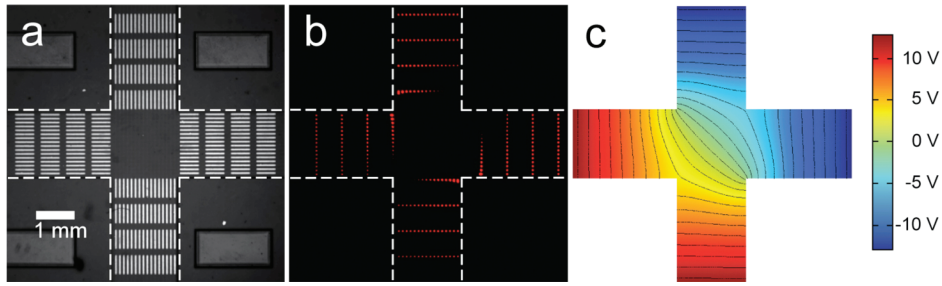

Figure 2. (a) Optical micrograph of the 2D microfluidic channel showing the positions of the four BPE electrode arrays. Each array consists of four columns, with 16 BPEs per column. The individual BPEs are 500 μm long and 50 μm wide. The channel dimensions are given in Scheme 1. The channels are filled with an aqueous, air-saturated solution containing 5.0 mM $Ru(bpy)_3^{2+}$ and 25.0 mM TPrA in 0.1 M phosphate buffer (pH 6.9). (b) False-color luminescence micrograph showing ECL emission from the BPE arrays when $E_{tot1} = E_{tot2} = 45$ V. (c) COMSOL Multiphysics simulation showing the potential gradient within the microfluidic channels. Both contour and surface plots represent the potential gradient in the device. The isopotential lines of the contour plot correspond to 1 V. Complete details regarding the simulation are provided in the Supporting Information.

geometrically constant, the location of the ECL emission is localized on different sections of the 2D-BPE. For example, when $E_{tot1} =$ 17.3 V and $E_{tot2} = 10.0$ V, the light emission moves to the upper-right edge of the BPE (Figure 1c). Likewise, when E_{tot1} and E_{tot2} are changed to the values shown in the caption of parts d−f of Figure 1, light emission moves counter-clockwise around the perimeter of the BPE. A movie, from which the frames in Figure 1 are extracted, is provided in the Supporting Information, and it shows that ECL emission can be moved around the entire perimeter of the BPE. The Supporting Information (Figure S1) also provides an analysis of the potential gradients corresponding to the results in Figure 1.

To better understand the electric field distribution in the vicinity of the channel intersection, the single BPE shown in Figure 1a was replaced with an array of BPEs (Figure 2a). In this case, each electrode in the array experiences a different value of ΔE_{elec}, depending on its position, and therefore the ECL intensity provides a map of the field gradient. In the optical micrograph shown in Figure 2a, the lighter regions are the Au BPEs and the dashed white lines delineate the walls of the PDMS microfluidic channels. Figure 2b is a luminescence micrograph obtained in the same region of the microfluidic device shown in Figure 2a when $E_{tot1} = E_{tot2} =$ 45.0 V. The intensity and location of the emission of red light from the anodic poles of the BPEs reflect the magnitude of ΔE_{elec} between the solution and each BPE: more intense emission covering more of the BPE indicates a higher value of the electric field in that region of the channel.[4] Figure S2 in the Supporting Information shows that the ECL intensity from the array is diminished when E_{tot1} and E_{tot2} are both lowered to 40, 35, and 30 V.

The experimental results in Figures 2b can be compared to finite element simulations of the potential gradient formed when symmetric potentials are applied across the two channels (Figure 2c). The simulations indicate that the highest gradients are at the corners connecting oppositely polarized channels. Likewise, the lowest potential differences occur near similarly polarized channels. Comparison of the simulated results with the luminescence micrograph in Figure 2b indicates a clear correspondence. Specifically, the simulations indicate that a sufficiently high value of ΔE_{elec} exists to illuminate 13 electrodes in the first rank of each of the four 16 × 4 electrode arrays. Experimentally, 11 of the 16 electrodes emit detectable light. This is reasonable agreement given that the simulations do not take into account the finite height of the channels and BPEs, transient effects resulting from the applied potentials and the available current, or the depolarization effect of the BPE array on the potential drop in the channel.[4] Note also that the ECL intensity is highest from those electrodes predicted by the simulations to have the highest value of ΔE_{elec}. Additional details about the simulations are provided in the Supporting Information.

To summarize, we have shown that particular locations on the perimeter of a BPE can be electrochemically isolated using a 2D electric field manipulated within the context of crossed microfluidic channels. Moreover, a map of ECL emission from an array of BPEs is in semiquantitative agreement with simulations of the electric field near the intersection of the channels. Because the 2D-BPE geometry makes it possible to control the potential difference between the solution and electrode at selected locations, one can imagine adapting this approach for applications such as electrochemical sensing, electrochemical synthesis of graded materials,[8] and high-throughput screening of electrocatalytic activity. Reports related to these applications will be forthcoming.

Acknowledgment. We gratefully acknowledge support from the Chemical Sciences, Geosciences, and Biosciences Division, Office of Basic Energy Sciences, Office of Science, U.S. Department of Energy (Contract No. DE-FG02-06ER15758). Funding for this project was also provided by the U.S. Army Research Office (grant no. W911NF-07-1-0330) and the U.S. Defense Threat Reduction Agency. We also thank the Robert A. Welch Foundation (Grant F-0032). B.-Y.C. was partially supported by a Korea Research Fund Grant funded by the Korean Government (KRF-2008-357-C00091).

Supporting Information Available: Information about materials, fabrication procedures, instrumentation, a movie showing ECL localization, and simulation results. This material is available free of charge via the Internet at http://pubs.acs.org.

References

(1) Zhan, W.; Alvarez, J.; Crooks, R. M. *J. Am. Chem. Soc.* **2002**, *124*, 13265–13270.
(2) Chow, K.-F.; Mavré, F.; Crooks, R. M. *J. Am. Chem. Soc.* **2008**, *130*, 7544–7545.
(3) Chow, K.-F.; Mavré, F.; Crooks, J. A.; Chang, B.-Y.; Crooks, R. M. *J. Am. Chem. Soc.* **2009**, *131*, 8364–8365.
(4) Mavré, F.; Chow, K.-F.; Sheridan, E.; Chang, B.-Y.; Crooks, J. A.; Crooks, R. M. *Anal. Chem.* **2009**, *81*, 6218–6225.
(5) Ulrich, C.; Andersson, O.; Nyholm, L.; Björefors, F. *Angew. Chem., Int. Ed.* **2008**, *47*, 3034–3036.
(6) Ulrich, C.; Andersson, O.; Nyholm, L.; Björefors, F. *Anal. Chem.* **2009**, *81*, 453–459.
(7) Duval, J. F. L.; Huijs, G. K.; Threels, W. F.; Lyklema, J.; van Leeuwen, H. P. *J. Colloid Interface Sci.* **2003**, *260*, 95–106.
(8) Ramakrishnan, S.; Shannon, C. *Langmuir* **2010**, *26*, 4602–4606.
(9) Bradley, J. C.; Ma, Z. M. *Angew. Chem., Int. Ed.* **1999**, *38*, 1663–1666.
(10) Bard, A. J. *Electrogenerated Chemiluminescence*; Marcel Dekker, Inc.: New York, 2004.

JA103667Y